REPORT DOCUMENTATION PAGE

Form Approved OMB NO. 0704-0188

1. REPORT DATE (DD-MM-YYYY)	2. REPORT TYPE	3. DATES COVERED (From - To)
	New Reprint	-

4. TITLE AND SUBTITLE
M13 bacteriophage-polymer nanoassemblies as drug delivery vehicles

5a. CONTRACT NUMBER
W911NF-09-1-0236

5b. GRANT NUMBER

5c. PROGRAM ELEMENT NUMBER
611102

6. AUTHORS
Nisaraporn Suthiwangcharoen, Tao Li, Kai Li, Preston Thompson, Shaojin You, Qian Wang

5d. PROJECT NUMBER

5e. TASK NUMBER

5f. WORK UNIT NUMBER

7. PERFORMING ORGANIZATION NAMES AND ADDRESSES
University of South Carolina Research Foundatio
South Carolina Research Foundation
901 Sumter ST, 5th floor Byrnes
Columbia, SC 29208 -0001

8. PERFORMING ORGANIZATION REPORT NUMBER

9. SPONSORING/MONITORING AGENCY NAME(S) AND ADDRESS(ES)
U.S. Army Research Office
P.O. Box 12211
Research Triangle Park, NC 27709-2211

10. SPONSOR/MONITOR'S ACRONYM(S)
ARO

11. SPONSOR/MONITOR'S REPORT NUMBER(S)
56056-CH.9

12. DISTRIBUTION AVAILIBILITY STATEMENT
Approved for public release; distribution is unlimited.

13. SUPPLEMENTARY NOTES
The views, opinions and/or findings contained in this report are those of the author(s) and should not contrued as an official Department of the Army position, policy or decision, unless so designated by other documentation.

14. ABSTRACT
Poly(caprolactone-b-2-vinylpyridine) (PCL–P2VP) coated with folate-conjugated M13 (FA–M13) provides a nanosized delivery system which is capable of encapsulating hydrophobic antitumor drugs such as doxorubicin (DOX). The DOX-loaded FA–M13–PCL–P2VP assemblies had an average diameter of approximately 200 nm and their structure was characterized using transmission electron microscopy, scanning electron microscopy, and dynamic light scattering. The particles were stable at physiological pH but could be degraded at a lower pH. The

15. SUBJECT TERMS
Bacteriophage M13, nanoassemblies, doxorubicin, drug delivery, polymer

16. SECURITY CLASSIFICATION OF:			17. LIMITATION OF ABSTRACT	15. NUMBER OF PAGES	19a. NAME OF RESPONSIBLE PERSON
a. REPORT	b. ABSTRACT	c. THIS PAGE			Qian Wang
UU	UU	UU	UU		19b. TELEPHONE NUMBER: 803-777-8436

Report Title

M13 bacteriophage-polymer nanoassemblies as drug delivery vehicles

ABSTRACT

Poly(caprolactone-b-2-vinylpyridine) (PCL–P2VP) coated with folate-conjugated M13 (FA–M13) provides a nanosized delivery system which is capable of encapsulating hydrophobic antitumor drugs such as doxorubicin (DOX). The DOX-loaded FA–M13–PCL–P2VP assemblies had an average diameter of approximately 200 nm and their structure was characterized using transmission electron microscopy, scanning electron microscopy, and dynamic light scattering. The particles were stable at physiological pH but could be degraded at a lower pH. The release of DOX from the nanoassemblies under acidic conditions was shown to be significantly faster than that observed at physiological pH. In addition, the DOX-loaded FA–M13–PCL–P2VP particles showed a distinctly greater cellular uptake and cytotoxicity against folate-receptor-positive cancer cells than folatereceptor-negative cells, indicating that the receptor facilitates folate uptake via receptor-mediated endocytosis. Furthermore, the DOX-loaded particles also had a significantly higher tumor uptake and selectivity compared to free DOX. This study therefore offers a new way to fabricate nanosized drug delivery vehicles.

REPORT DOCUMENTATION PAGE (SF298)
(Continuation Sheet)

Continuation for Block 13

ARO Report Number 56056.9-CH
M13 bacteriophage-polymer nanoassemblies as ...

Block 13: Supplementary Note

Approved for public release; distribution is unlimited.

Nano Res. 2011, 4(5): 483–493
DOI 10.1007/s12274-011-0104-2
Research Article

ISSN 1998-0124
CN 11-5974/O4

M13 Bacteriophage–Polymer Nanoassemblies as Drug Delivery Vehicles

Nisaraporn Suthiwangcharoen[1], Tao Li[1], Kai Li[1], Preston Thompson[1], Shaojin You[2] (✉), and Qian Wang[1] (✉)

[1] Department of Chemistry and Biochemistry and Nanocenter, University of South Carolina Columbia, SC 29208, USA
[2] Histo-Pathology Core, Atlanta VA Medical Center, 1670 Clairmont Road, Decatur, GA 30033, USA

Received: 8 October 2010 / Revised: 10 December 2010 / Accepted: 6 January 2011

ABSTRACT

Poly(caprolactone-*b*-2-vinylpyridine) (PCL–P2VP) coated with folate-conjugated M13 (FA–M13) provides a nanosized delivery system which is capable of encapsulating hydrophobic antitumor drugs such as doxorubicin (DOX). The DOX-loaded FA–M13–PCL–P2VP assemblies had an average diameter of approximately 200 nm and their structure was characterized using transmission electron microscopy, scanning electron microscopy, and dynamic light scattering. The particles were stable at physiological pH but could be degraded at a lower pH. The release of DOX from the nanoassemblies under acidic conditions was shown to be significantly faster than that observed at physiological pH. In addition, the DOX-loaded FA–M13–PCL–P2VP particles showed a distinctly greater cellular uptake and cytotoxicity against folate-receptor-positive cancer cells than folate-receptor-negative cells, indicating that the receptor facilitates folate uptake via receptor-mediated endocytosis. Furthermore, the DOX-loaded particles also had a significantly higher tumor uptake and selectivity compared to free DOX. This study therefore offers a new way to fabricate nanosized drug delivery vehicles.

KEYWORDS

Bacteriophage M13, nanoassemblies, doxorubicin, drug delivery, polymer

1. Introduction

The development of nanosized targeted drug delivery vehicles in cancer chemotherapy in order to improve the effectiveness of drug delivery vehicles while minimizing toxic effects on normal cells has attracted great attention in the past decades [1–6]. Unfortunately, problems such as toxicity, stability, and immunoresistance remain potential concerns [4]. Recently, there has been increased interest in the use of viruses or bacteriophages as nanotemplates for biomaterial [7–13] and biomedical studies [14–18]. Viruses and bacteriophages have well-defined structures and can be easily modified with different functional units [19–22]. In particular, they offer a polyvalent ligand-display scaffold that can enhance the cell targeting efficiency towards tumor cells [15, 19, 23, 24]. More importantly, several viruses and bacteriophages appear to be safe and non-toxic based on the results from *in vivo* studies [14, 25, 26]. Our group has previously reported that core–shell nanoassemblies of virus or virus-like particles and copolymers can be readily formed with controllable size distribution [27–30]. Herein, we demonstrate that the assembly of the

Address correspondence to Qian Wang, wang@mail.chem.sc.edu; Shaojin You, shaojin.you@va.gov

folate-grafted filamentous bacteriophage M13 with the copolymer poly(caprolactone-*b*-2-vinylpyridine) (PCL–P2VP), a biodegradable polymer, can serve as a potential scaffold for drug delivery.

M13 is a filamentous bacteriophage with a single strand deoxyribonucleic acid (DNA) genome 6,407 nucleotides long, enclosed by 2,700 copies of the major coat protein P8 [31–34]. M13 can be inexpensively purified in large quantity and has been employed extensively in many applications ranging from functional materials to novel biomedical applications [19, 35, 36]. The structure of the M13 bacteriophage is well-defined and can be genetically engineered to produce conductive fibers [35] or display peptides or proteins in controlled orientations [31, 36, 37]. Additionally, a variety of functionalities, including drugs [19, 38–41], arginine–glycine–aspartic (RGD) peptides [36], and fluorescent dyes [42, 43], can be chemically anchored on the surface of M13 bacteriophage. Our group has systematically investigated the bioconjugation chemistry of M13, and used such modified M13 phages to produce conductive nanofibers [35], direct cell growth [36], and target cancer cells [44]. More importantly, recent human clinical trials have reported that bacteriophage M13 can cross the blood-brain barrier and does not exhibit significant toxicity or immune response in humans [45], which highlights the potential application of M13 bacteriophage in drug delivery.

In this paper, M13 bacteriophage was used together with a block copolymer, PCL–P2VP, to form core–shell nanoassemblies, which can entrap hydrophobic drugs as depicted in Fig. 1. In order to specifically target cancer cells, folic acid was used to conjugate to *N*-terminal and/or surface lysine residues of M13 as described previously [44]. It is well known that

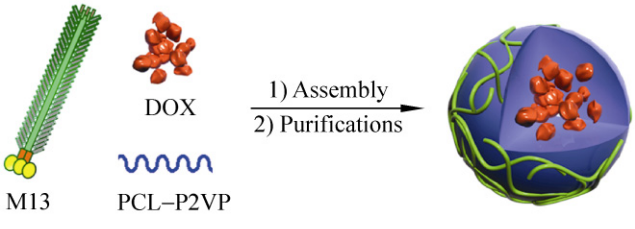

Figure 1 Schematic illustration of the formation of DOX-loaded M13–PCL–P2VP nanoassemblies

several malignant tissues over-express the folate receptor [46, 47]. Using M13 as carrier, folate moieties can cluster on the surface of M13 with control over the spacing and orientation, which allows for multivalent target–receptor interactions, a principle of polyvalency [48], and can improve the binding and targeting significantly. PCL–P2VP was chosen because it contains a biodegradable hydrophobic block (PCL) and a polar, hydrogen bonding, pH-sensitive block (P2VP) [49, 50]. Moreover, it has been reported that PCL–P2VP can be used in drug encapsulation [49]. In the final core–shell structure, the PCL–P2VP copolymer comprises the core and the folate-conjugated M13 forms the shell, incorporated with doxorubicin (DOX) as a prototypical antitumor drug. KB cells (a human nasopharyngeal cell line) overexpressing folate receptors were used to evaluate the *in vitro* malignant cell uptake [46, 47, 51], while human mesenchymal stem cells (HMSCs), which lack folate receptors, were used as a negative control.

2. Results and discussion

2.1 Synthesis and characterization of the FA–M13–PCL–P2VP nanoassemblies

It has been reported that the modification of nanoparticles with folic acid is one of the strategies to enhance specific cellular uptake via receptor-mediated endocytosis [46]. In order to enhance the interaction between the particle and cells, folic acid was chosen to conjugate to the M13 via the *N*-ethyl-*N*′-(3-dimethylaminopropyl)carbodiimide hydrochloride (EDC) coupling reaction as depicted in Fig. 2. The folate-conjugated M13 (FA–M13) was prepared and characterized as previously described [44, 52]. A successful folate-conjugated M13 was analyzed using matrix-assisted laser desorption mass spectrometry (MALDI–MS), and the results showed that the molecular mass of the folic acid- modified M13 subunit was 5,663 *m*/*z*, while the unmodified M13 subunit was 5,238 *m*/*z* (Fig. 2), which indicated that the majority of the modified protein subunits are mono-derivatized with folic acid. Folic acid contains two carboxylic acid groups and it is difficult to identify the reactive one in our study. However, similar studies reported in the

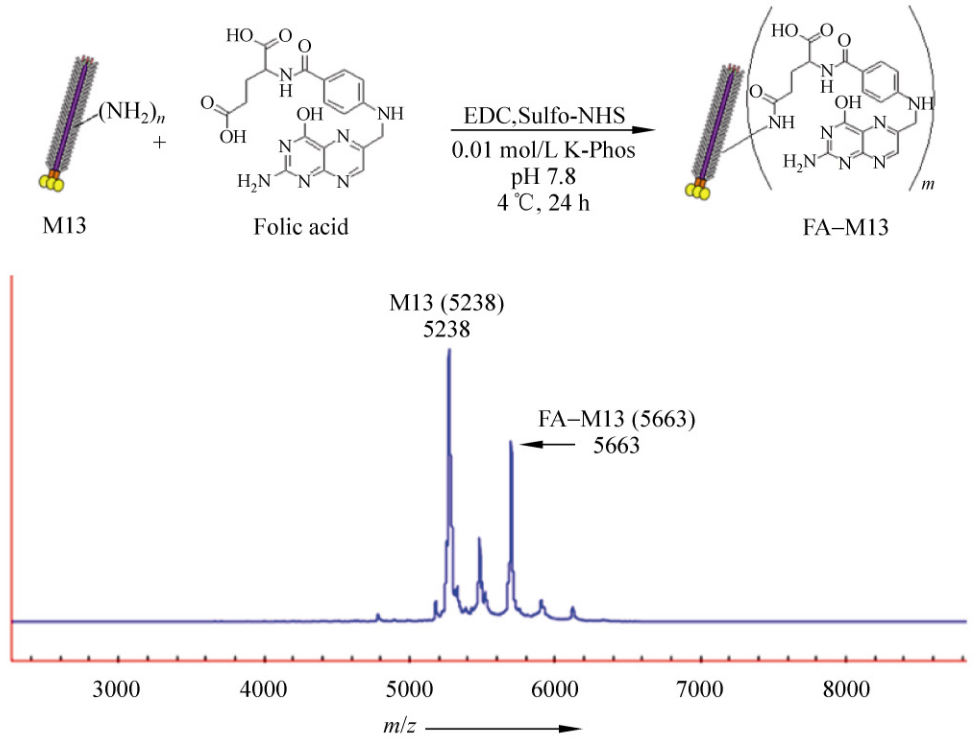

Figure 2 Schematic illustration of the conjugation of folic acid to M13. Folic acid, activated with EDC and *N*-hydroxysuccinimide (NHS), was coupled to M13 resulting in stable FA–M13 particles. MALDI–MS data showed that the molecular mass of the unmodified M13 subunit was 5,238 *m*/*z*, and the mass of FA–M13 was 5,663 *m*/*z*

literature have suggested that the carboxylic group at the γ position is more sterically accessible towards carbodiimide activated amidation reactions [53].

DOX-loaded nanoassemblies were then prepared by the following method: DOX·HCl, dissolved in dimethylformamide (DMF) containing triethylamine, was pre-mixed with a tetrahydrofuran (THF) solution containing PCL–P2VP before it was added dropwise to the aqueous solution containing FA–M13. The solution was vigorously stirred at room temperature overnight, and the samples were purified via filtration and centrifugation to remove unloaded DOX and free M13 particles. The transmission electron microscopy (TEM) image of DOX-loaded particles before purification is shown in Fig. 3(a). After the particles were purified (by filtration and centrifugation), less free M13 was observed in solution and resulted in a more homogenous particle surface, while the size of the particles remained approximately the same (Figs. 3(b) and 3(c)). As visualized by TEM and scanning electron microscopy (SEM), the DOX-loaded FA–M13–PCL–P2VP had a spherical shape with a mean size of 200–250 nm. This result is consistent with that obtained by dynamic light scattering (DLS) measurements (Fig. 3(d)), which was 221 nm ± 64 nm. The size of the particle can be controlled by altering the mass ratio of M13 to the polymer. Generally, the size of the particles increased as the polymer concentration increased. The size distribution remained narrow even when the particle size was increased. However, smaller particle sizes are preferable because they can be more efficiently taken up by cells.

With the encapsulation of DOX into the particle, we found that the loading of DOX did not have a significant influence on the morphology, zeta potential, size, or size distribution of FA–M13–PCL–P2VP particles, but more aggregation was observed. The encapsulation efficiency (EE) and loading capacity (LC) were also investigated. The EE represents the percentage of DOX loaded in particles with respect to

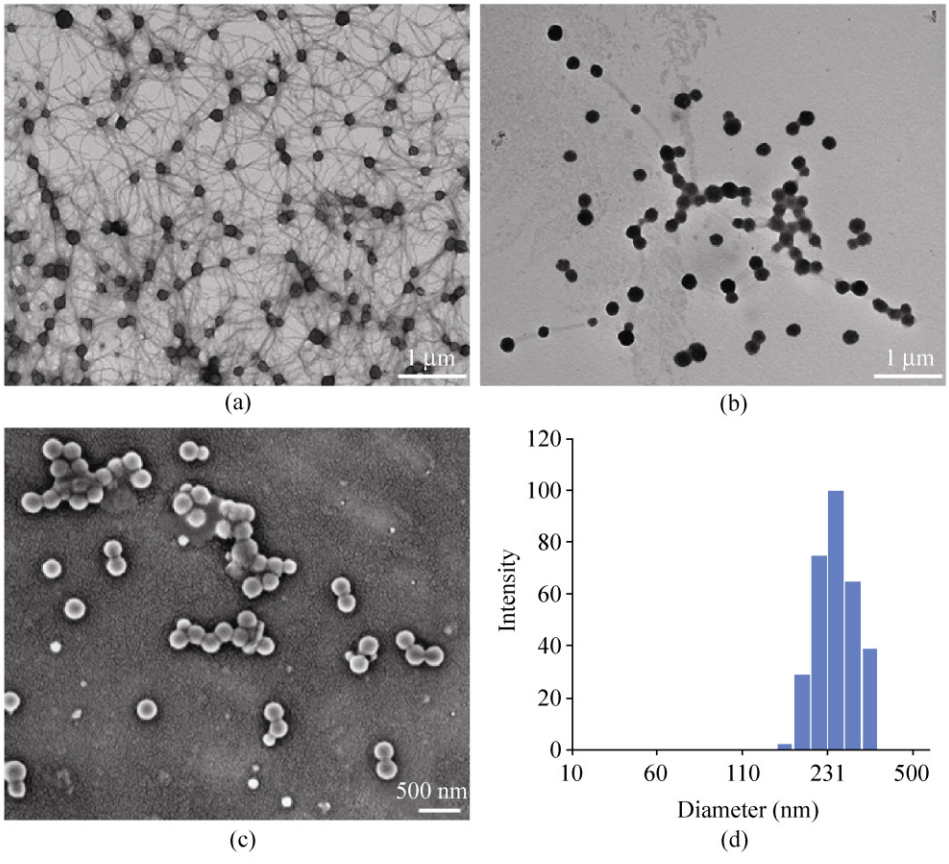

Figure 3 TEM images of DOX-loaded M13–PCL–P2VP taken (a) before and (b) after purification. Less free M13 particles were observed after the purification resulted in cleaner core–shell assemblies. (c) Field emission SEM (FESEM) image of the spherical nanoassemblies after purification. (d) Particle size and size distribution from DLS. The removal of excess M13 had no effect on the overall size of the particles

the initial amount of DOX used to prepare the DOX-loaded particles, which was 49 wt.% ± 2 wt.%, while the LC is expressed as a percentage of the amount of loaded-DOX relative to the amount of nanoparticles, which was 11 wt.% ± 0.5 wt.%. The reproducibility of the EE and LC values was satisfactory, showing narrow variation with a low standard deviation (data not shown).

Additionally, the surface charge properties of the nanoassemblies were evaluated after removing the excess M13 from the solution [54, 55]. As shown in Table 1, the zeta potential value increased upon the assembly of M13 or FA–M13 and polymer as compared to the pure M13 or FA–M13 under the same pH conditions. Loading of DOX into the particles did not significantly affect the zeta potential value of the particles. As reported in the literature, if the zeta potential value is greater than 30 mV, the particles are generally considered stable regardless of the charge type [56]. These results indicated that the polymer–M13 assemblies were relatively stable, which was also confirmed using TEM, which showed that the nanoassemblies were stable for up to 4 weeks at a storage temperature of 2–8 °C. DOX-loaded FA–M13–PCL–P2VP, however, was stable at room temperature for about 1–2 weeks, after which time precipitation was

Table 1 Zeta potential values of M13, FA–M13, and particles. All values are mean standard ± deviation for nanoassemblies prepared in triplicate

Sample (pH 7.8)	ζ (mV)
M13	–22.64 ± 1.58
FA–M13	–25.62 ± 0.78
M13–PCL–P2VP	–36.25 ± 1.92
FA–M13–PCL–P2VP	–32.79 ± 1.28
DOX–FA–M13–PCL–P2VP	–30.35 ± 2.05

evident. After analyzing the samples by TEM, spherical particles were still observed. The results suggest that DOX may slowly diffuse out and precipitate in the aqueous solution.

2.2 *In vitro* DOX release from pH-sensitive particles

The pH-dependent DOX release profiles from the pH-responsive M13–PCL–P2VP were examined by dialysis against buffer at different pH values (Fig. 4). For the DOX-loaded particles, beyond the initial burst, a slower release of the drug was observed at approximately 9 h resulting in a sustained drug release in comparison to the rapid release of unloaded DOX. The DOX release rate at pH 5.0 was faster, with greater than 70% released within 12 h, indicating the pH-sensitive nature of FA–M13–PCL–P2VP assemblies [57, 58]. In addition, no spherical particles were observed by TEM after dialysis against buffer at pH 5. The burst release of DOX was observed within 2 h when free DOX was used. We rationalize that with the decrease of pH of the external environment, the pyridine units in PCL–P2VP are protonated and thus lead to the deformation of the particles and allow a rapid release of DOX to the external environment.

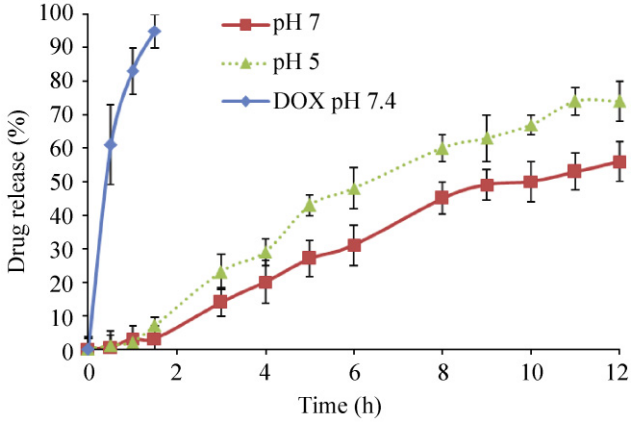

Figure 4 Drug release profiles of DOX-loaded M13–PCL–P2VP at different pH. DOX solution was used as a control

2.3 Cellular uptake of DOX from pH-sensitive particles

In order to investigate the selective targeting ability of the particles, KB cells and HMSCs were employed as folate receptor positive (FR+) cells and folate receptor negative (FR–) cells, respectively. The intracellular localization of free DOX and DOX-loaded M13–PCL–P2VP was visualized using confocal laser scanning microscopy. For KB cells, the cellular uptake of DOX was significantly higher in FA–M13–PCL–P2VP compared with M13–PCL–P2VP due to folate receptor-mediated endocytosis (Fig. 5(a)). For free DOX, red fluorescence was observed only in nuclei, whereas for DOX-loaded particles the signal was found in both cytoplasm and nuclei. After 24 h, most of the nanoassembly-derived DOX molecules were distributed in the cell nuclei in a similar manner to that of free DOX, resulting in stronger DOX fluorescence (Fig. 5(b)). The rapid accumulation of DOX-loaded FA–M13–PCL–P2VP in the cells is likely to occur via folate receptor-mediated endocytosis due to the presence of folate receptors on the surface of KB cells [47, 48].

The distribution of DOX in HMSCs was also examined. Due to the lack of folate receptors, HMSCs displayed a weak fluorescence signal after incubating with either M13–PCL–P2VP or FA–M13–PCL–P2VP. This observation suggests that there was less cellular uptake of particles in HMSCs compared to KB cells, and the folate-conjugated M13–PCL–P2VP has the ability to specifically target folate receptor-overexpressed tumor cells for the delivery of therapeutics and imaging motifs.

The results of cellular uptake of DOX-loaded particles were further confirmed by cell sorting analysis. After the cells were incubated with the particles at 37 ˚C for 24 h, they were extensively washed, detached, and then subjected to flow cytometry. The blank cells were used as controls. As depicted in Fig. 5(c), KB cells exhibited a higher uptake of DOX-loaded FA–M13–PCL–P2VP than HMSCs, indicating the selective targeting of the particles. Notably, KB cells also showed a higher uptake of DOX-loaded FA–M13–PCL–P2VP than of free DOX, which is consistent with the observations obtained from confocal microscopy analysis (Figs. 5(a) and 5(b)). Again, the presence of folate units on the surface of the assemblies facilitated the cell uptake. If the particles cannot be endocytosed by cells, they will remain in the interstitial space [59], which will be removed after several washes with phosphate buffered saline (PBS) buffer.

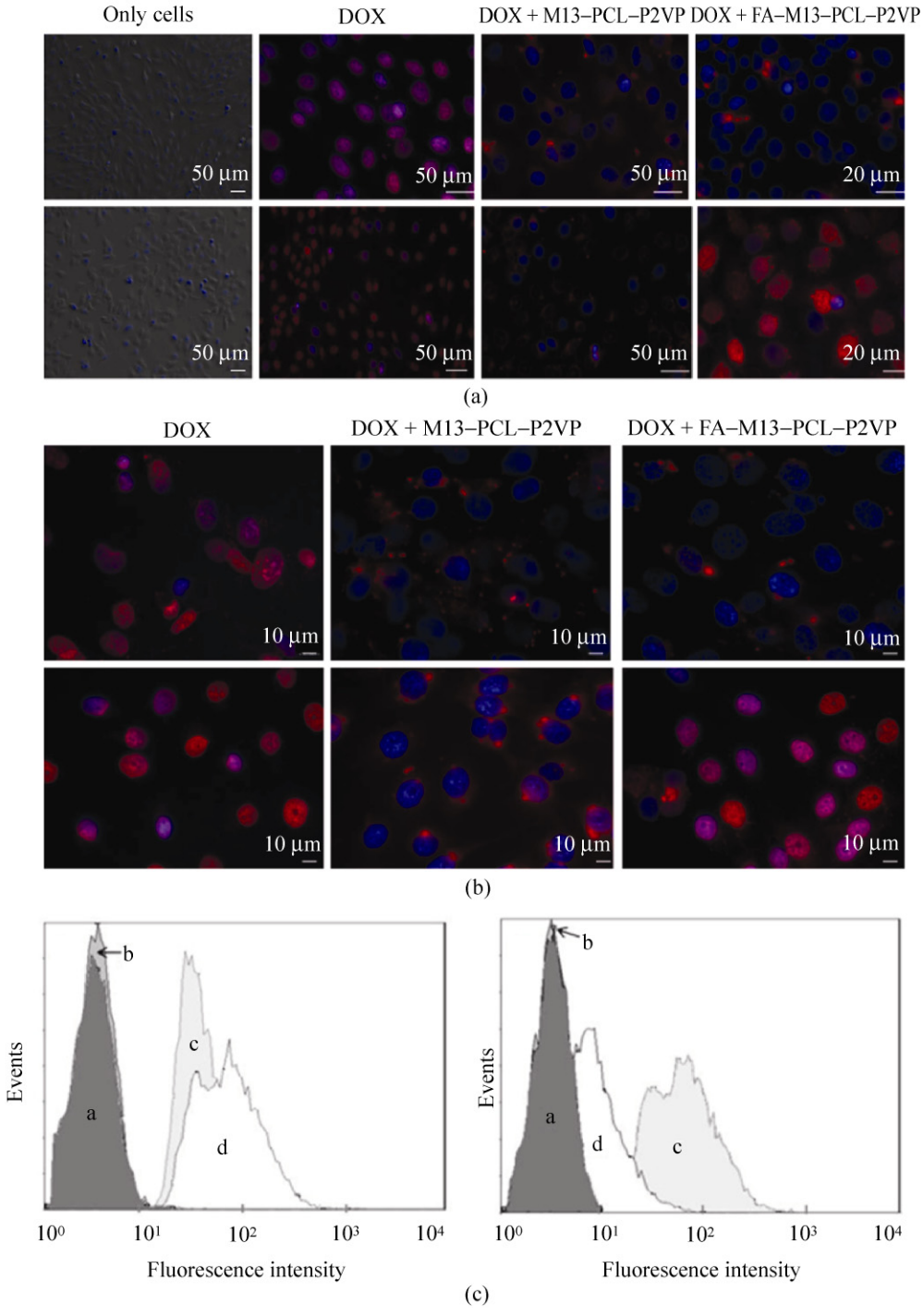

Figure 5 Confocal microscopic images of HMSCs and KB cells incubated with DOX, DOX-loaded M13–PCL–P2VP, and DOX-loaded FA–M13–PCL–P2VP at an equivalent DOX concentration of 1 μg/mL at 37 ˚C after 2 h (a) and 24 h (b). The blue nuclei of cells were stained with 4'-, 6-diamidino-2-phenylindole (DAPI). (c) Shows a flow cytometric analysis of KB cells (left) and HMSCs (right) incubated at 37 ˚C for 24 h with (a) no treatment, (b) DOX-loaded M13–PCL–P2VP, (c) unloaded DOX, and (d) DOX-loaded FA–M13–PCL–P2VP. The concentration of DOX was 1 μg/mL

2.4 Cytotoxicity studies

The cytotoxicity effects of DOX-loaded nanoassemblies were evaluated using KB cells and HMSCs via CellTiter-Blue Cell Viability Assay. Both types of cells were treated with blank M13–PCL–P2VP, free DOX, and DOX-loaded M13–PCL–P2VP for 24 h with an equivalent concentration of DOX. As shown in Fig. 6, both the KB cells and HMSCs displayed high cell viability while grown with the unloaded particles, indicating that the particles are not toxic to the cells. On the other hand, both cells showed indistinguishable cell viabilities when treated with free DOX. DOX-loaded FA–M13–PCL–P2VP showed a higher cytotoxicity compared to free DOX towards KB cells. However, the same particles showed less cytotoxicity against HMSCs, thereby demonstrating the selective cytotoxicity of the DOX-loaded FA–M13–PCL–P2VP particles. These results demonstrated the high selectivity of FA–M13 decorated particles, as well as the ability to effectively deliver therapeutic agents.

3. Experimental

3.1 Materials

Doxorubicin hydrochloride (DOX·HCl) was obtained from Zhejiang Sunrise Fine Chemicals Co., Ltd. The PCL–P2VP copolymer was from Polymer Source, Inc., with M_n (P2VP) = 20,900, M_n (PCL) = 35,400, and M_w/M_n = 1.8. NHS, EDC, and folic acid were purchased from VWR Scientific. Solutions of resazurin were purchased from Promega as the CellTiter-Blue Cell Viability Assay kit, and were used according to the manufacturer's instructions. RPMI 1640 without folic acid and Dulbecco's Modified Eagle's Medium (DMEM) were purchased from Invitrogen (Carlsbad, CA). KB cells and HMSCs were obtained from ATCC. Triethylamine was dried by distillation over potassium hydroxide prior to use. Potassium phosphate buffer (0.01 mol/L, pH 7.8) was used throughout the experiments unless otherwise specified. TEM analyses were carried out by depositing 10 μL of sample onto a 100-mesh carbon-coated copper grid for 5 min. The grid was then stained with 10 μL of 2% uranyl acetate and visualized with a Hitachi H-800 TEM electron microscope. For the SEM analyses, the sample was dried overnight and coated with gold, and the images recorded using a Quanta 200 Environmental Scanning Electron Microscope (ESEM, Quanta 200 FEI). DLS analysis was performed using a submicron particle sizer (Autodilute^{PAT} Model 370). Fluorescent microcopy was performed on Olympus IX 86. MALDI–MS analysis was performed using a Bruker Ultraflex I time-of-flight (TOF)/TOF mass spectrometer. The particle charge was measured as zeta potential using a Z-Potential Analyzer (Brookhaven Instruments Corporation). The measurement was performed after dilution of the particles with nanopure water to reach the maximum requirement of the instrument.

3.2 Preparation and characterization of folate-conjugated M13 (FA–M13)

The carboxylate group of folic acid was activated by NHS and EDC as described earlier [52, 60, 61]. Briefly,

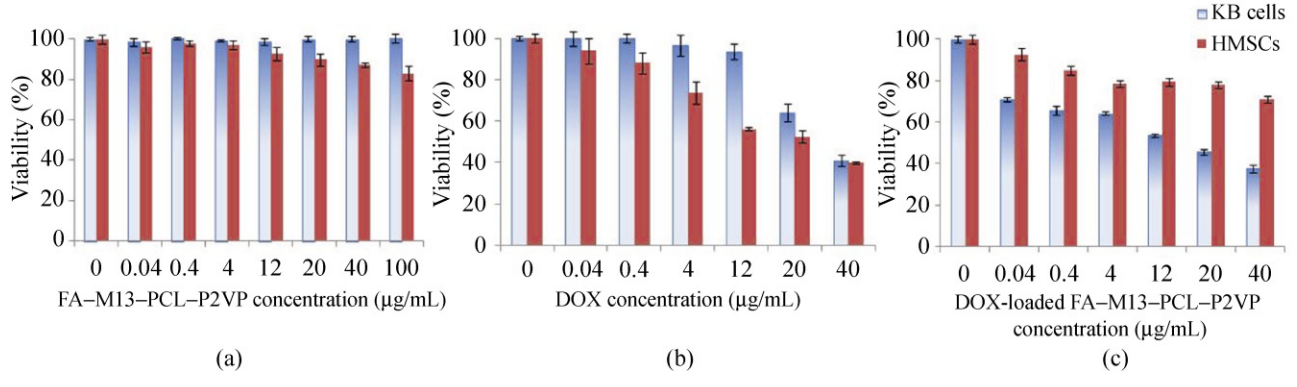

Figure 6 Cytotoxicity assays of (a) FA–M13–PCL–P2VP particles, (b) DOX, and (c) DOX-loaded FA–M13–PCL–P2VP. The cells were exposed to DOX for 24 h

a solution of folic acid, EDC, and sulfo-NHS (in a molar ratio of 1:1.1:2.5) in anhydrous dimethylsulfoxide (DMSO) (1 mL) was prepared and stirred in the dark at room temperature for 30 min. The activated folic acid solution (200 μL) was then added to a viral suspension in 1 mL buffer. Following an overnight incubation at 4 °C, the reaction mixture was dialyzed against buffer for 48 h to remove excess free folic acid. The successful folate-conjugated M13 was analyzed using MALDI–TOF. A solution of M13 (1 mg/mL, 24 μL) was denatured by incubating with guanidinium chloride (6.0 mol/L, 6 μL) for 5 min at room temperature. Millipore ZipTip-C18® tips were used to remove salts. The denatured protein was spotted onto a MALDI plate and subjected to analysis by a Bruker Ultraflex I TOF/TOF mass spectrometer. MS grade 2,5-dihydroxybenzoic acid with 0.1% TFA was used as the matrix.

3.3 Preparation and characterization of DOX-loaded M13–PCL–P2VP

Doxorubicin hydrochloride (1 mg) in 1 mL of DMF was stirred with 3 equiv. of triethylamine in the dark at room temperature for 2 h to obtain a DOX base. The DOX base solution (125 μL) was then mixed with a solution of PCL–P2VP in THF (2 mg/mL, 125 μL). Then, a premixed DOX solution in polymer was slowly added to a solution of FA–M13 in buffer and stirred overnight. The mass ratio of M13 to PCL–P2VP was 1:5, whereas the solvent ratio of buffer to THF was 19:1. Free DOX was removed from FA–M13–PCL–P2VP by filtration through a 0.2 μm syringe filter. The particles were further purified via centrifugation at 10,000 r/min for 7 min. This step was repeated several times, and the final pellet was resuspended in buffer as the final product. DOX-loaded M13–PCL–P2VP was then quantified photometrically at 488 nm, using an extinction coefficient of 11,500 $L \cdot mol^{-1} \cdot cm^{-1}$. The EE and the LC were calculated by equation (1) and (2), respectively, assuming that there was no mass loss during purification

$$EE = (a - b)/a \quad (1)$$

$$LC = (a - b)/c \quad (2)$$

where a is the total mass of initial DOX in solution, b is mass of free DOX, and c is the mass of FA–M13–PCL–P2VP [62].

3.4 DOX release experiments

Free DOX and DOX-loaded particles were transferred to a dialysis tube (cut-off molecular mass: 3500 Da) and immersed in a tube containing phosphate buffered saline (PBS; pH 7.4) or 0.1 mol/L acetate buffer (pH 5.0) at 37 °C while stirring gently. At specific time intervals, aliquots of the solution in the dialysis bag were withdrawn and subjected to photometrical assay at 485 nm. Fresh medium was replaced after every measurement. The experiment was performed in triplicate, and the average value is reported.

3.5 Cell culture

KB cells, which overexpress folate receptors, and HMSCs, which lack folate receptors, were used in the study. KB cells were maintained in RPMI 1640 medium without folic acid, and with 10% fetal bovine serum (FBS) and 1% penicillin/streptomycin [46, 47]. HMSCs were grown in DMEM supplemented with 10% FBS and 1% penicillin/streptomycin. Cells were grown at 37 °C with 5% CO_2. Cells were plated at a density of 1.5×10^4 cell/mL, 24 h prior to the experiment. Then the medium was replaced with 1 mL of fresh medium containing (a) DOX, (b) DOX-loaded M13–PCL–P2VP, or (c) DOX-loaded FA–M13–PCL–P2VP while maintaining a constant DOX concentration. After 24 h, the growth medium was removed, and cells were washed three times with PBS. After fixation in 4% paraformaldehyde in PBS for 20 min at room temperature, cells were washed three times with PBS again. Later, cells were stained with DAPI reagent for 10 min followed by several washes with PBS. Finally, cells were mounted on a microscope slide and visualized using a confocal microscope.

3.6 *In vitro* flow cytometry study

KB cells and HMSCs (1×10^6 cell/well) were cultured in a 6-well plate. After 24 h, the medium was replaced by fresh medium containing (a) DOX, (b) DOX-loaded M13–PCL–P2VP, or (c) DOX-loaded FA–M13–PCL–P2VP while maintaining a constant DOX concentration. After 24 h, the medium was removed, and cells were

washed three times with serum free medium. The cells were trypsinized, washed three times with PBS buffer, fixed with 4% paraformaldehyde, and washed three times with PBS buffer. After the cells were resuspended in fluorescence-activated cell sorting (FACS) buffer, cell fluorescence was measured by flow cytometry.

3.7 Cytotoxicity assay

Cell viability was determined using the conventional CellTiter-Blue assay. Briefly, each cell was seeded on a 96-well plate reader at a density of 1.5×10^4 cell/mL. After 24 h of incubation (37 ˚C, 5% CO_2), the medium was replaced with 100 μL of fresh medium containing various concentrations of samples. After 24 h of incubation, CellTiter-Blue solution (20 μL) was added to each well and incubated for another 4 h. The fluorescence was measured on a Spectramax Gemini EM spectrophotometer with an excitation wavelength of 560 nm and an emission wavelength of 590 nm.

4. Conclusion

We have successfully developed DOX-loaded pH-responsive FA–M13–PCL–P2VP nanoassemblies that are stable under physiological conditions but dissociated under an acidic environment. DOX-loaded particles show noticeable antitumor selectivity compared to free DOX. Reduced cellular uptake in HMSCs compared to KB cells demonstrates the selectivity of the particles. Our method of preparation of nanoassemblies provides a simple way of controlling particle size, encapsulating hydrophobic drugs, and targeting specific tumor cells. We believe that these features demonstrate that such nanoassemblies are attractive for the design of antitumor agents and can provide a new strategy for future *in vivo* use.

Acknowledgements

We are grateful for financial support from the US National Science Foundation (NSF) (CAREER program and No. DMR-0706431), US Department of Defense (DoD) (No. W911NF-09-1-0236), the Alfred P. Sloan Scholarship, the Camille Dreyfus Teacher–Scholar Award, DoD-Army Research Office (ARO), and the W. M. Keck Foundation. We are also indebted to Dr. Udai Singh for assistance with flow cytometry and Laying Wu for TEM and SEM analyses.

References

[1] Farokhzad, O. C.; Langer, R. Nanomedicine: Developing smarter therapeutic and diagnostic modalities. *Adv. Drug Deliver. Rev.* **2006**, *58*, 1456–1459.

[2] Farokhzad, O. C.; Langer, R. Impact of nanotechnology on drug delivery. *ACS Nano* **2009**, *3*, 16–20.

[3] Ferrari, M. Cancer nanotechnology: Opportunities and challenges. *Nat. Rev. Cancer* **2005**, *5*, 161–171.

[4] Kim, D. K.; Dobson, J. Nanomedicine for targeted drug delivery. *J. Mater. Chem.* **2009**, *19*, 6294–6307.

[5] Sinha, R.; Kim, G. J.; Nie, S. M.; Shin, D. M. Nanotechnology in cancer therapeutics: Bioconjugated nanoparticles for drug delivery. *Mol. Cancer Ther.* **2006**, *5*, 1909–1917.

[6] Zhang, L.; Gu, F. X.; Chan, J. M.; Wang, A. Z.; Langer, R.; Farokhzad, O. C. Nanoparticles in medicine: Therapeutic applications and developments. *Clin. Pharmacol. Ther.* **2008**, *83*, 761–769.

[7] Royston, E.; Ghosh, A.; Kofinas, P.; Harris, M. T.; Culver, J. N. Self-assembly of virus-structured high surface area nanomaterials and their application as battery electrodes. *Langmuir* **2007**, *24*, 906–912.

[8] Klem, M. T.; Young, M.; Douglas, T. Biomimetic synthesis of β-TiO_2 inside a viral capsid. *J. Mater. Chem.* **2008**, *18*, 3821–3823.

[9] Yi, H.; Rubloff, G. W.; Culver, J. N. TMV microarrays: Hybridization-based assembly of DNA-programmed viral nanotemplates. *Langmuir* **2007**, *23*, 2663–2667.

[10] Mao, C.; Aihua, L.; Binrui, C. Virus-based chemical and biological sensing. *Angew. Chem. Int. Ed.* **2009**, *48*, 6790–6810.

[11] Liu, A.; Abbineni, G.; Mao, C. Nanocomposite films assembled from genetically engineered filamentous viruses and gold nanoparticles: Nanoarchitecture- and humidity-tunable surface plasmon resonance spectra. *Adv. Mater.* **2009**, *21*, 1001–1005.

[12] Mao, C. B.; Flynn, C. E.; Hayhurst, A.; Sweeney, R.; Qi, J. F.; Georgiou, G.; Iverson, B.; Belcher, A. M. Viral assembly of oriented quantum dot nanowires. *Proc. Nat. Acad. Sci. U. S. A.* **2003**, *100*, 6946–6951.

[13] Mao, C. B.; Solis, D. J.; Reiss, B. D.; Kottmann, S. T.; Sweeney, R. Y.; Hayhurst, A.; Georgiou, G.; Iverson, B.; Belcher, A. M. Virus-based toolkit for the directed synthesis of magnetic and semiconducting nanowires. *Science* **2004**,

303, 213–217.

[14] Destito, G.; Yeh, R.; Rae, C. S.; Finn, M. G.; Manchester, M. Folic acid-mediated targeting of cowpea mosaic virus particles to tumor cells. *Chem. Biol.* **2007**, *14*, 1152–1162.

[15] Young, M.; Willits, D.; Uchida, M.; Douglas, T. Plant viruses as biotemplates for materials and their use in nanotechnology. *Ann. Rev. Phyt.* **2008**, *46*, 361–384.

[16] Kaur, G.; Valarmathi, M. T.; Potts, J. D.; Wang, Q. Plant virus as polyvalent substrate to promote the osteoblastic differentiation of rat bone marrow stromal cells. *Biomaterials,* **2008**, *29*, 4074–4081.

[17] Kaur, G.; Valarmathi, M. T.; Potts, J. D.; Jabbari, E.; Sabo-Attwood, T.; Wang, Q. Regulation of osteogenic differentiation of rat bone marrow stromal cells on 2D nanorod substrates. *Biomaterials,* **2010**, *31*, 1732–1741.

[18] Ngweniform, P.; Abbineni, G.; Cao, B. R.; Mao, C. B. Self-assembly of drug-loaded liposomes on genetically engineered target-recognizing M13 phage: A novel nanocarrier for targeted drug delivery. *Small* **2009**, *5*, 1963–1969.

[19] Lee, L. A.; Niu, Z.; Wang, Q. Viruses and virus-like protein assemblies—Chemically programmable nanoscale building blocks. *Nano Res.* **2009**, *2*, 349–364.

[20] Bruckman, M.; Kaur, G.; Lee, L. A.; Xie, F.; Sepulveda, J.; Breitenkamp, R.; Zhang, X.; Joralemon, M.; Russell, T. P.; Emrick, T.; Wang, Q. Surface modification of tobacco mosaic virus with "click" chemistry. *ChemBioChem* **2008**, *9*, 519–523.

[21] Barnhill, H. N.; Claudel-Gillet, S.; Ziessel, R.; Charbonniére, L. J.; Wang, Q. Prototype protein assembly as scaffold for time-resolved fluoroimmuno assays. *J. Am. Chem. Soc.* **2007**, *129*, 7799–7806.

[22] Wang, Q.; Lin, T.; Tang, L.; Johnson, J. E.; Finn, M. G. Icosahedral virus particles as addressable nanoscale building blocks. *Angew. Chem. Int. Ed.* **2002**, *114*, 477–480.

[23] Strable, E.; Finn, M. G. Chemical modification of viruses and virus-like particles. *Virus. Nanotechno.* **2009**, *327*, 1–21.

[24] Wang, Q.; Lin, T. W.; Johnson, J. E.; Finn, M. G. Natural supramolecular building blocks: Cysteine-added mutants of cowpea mosaic virus. *Chem. Biol.* **2002**, *9*, 813–819.

[25] Koudelka, K. J.; Rae, C.; Manchester, M. A plant-virus based nanoscaffold interacts specifically with the mammalian cell surface. *Nanomed.: Nanotechnol. Biol. Med.* **2007**, *3*, 349–350.

[26] Manchester, M. Targeted therapy using virus-based nanoparticles (VNPs). *Nanomed.: Nanotechnol. Biol. Med.* **2006**, *2*, 294.

[27] Li, T.; Niu, Z.; Emrick, T.; Russell, T. P.; Wang, Q. Core/shell biocomposites from the hierarchical assembly of bionanoparticles and polymer. *Small* **2008**, *4*, 1624–1629.

[28] Li, T.; Wu, L.; Suthiwangcharoen, N.; Bruckman, M. A.; Cash, D.; Hudson, J. S.; Ghoshroy, S.; Wang, Q. Controlled assembly of rodlike viruses with polymers. *Chem. Commun.* **2009**, 2869–2871.

[29] Li, T.; Ye, B.; Niu, Z.; Thompson, P.; Seifert, S.; Lee, B.; Wang, Q. Closed-packed colloidal assemblies from icosahedral plant virus and polymer. *Chem. Mater.* **2009**, *21*, 1046–1050.

[30] Li, T.; Niu, Z.; Suthiwangcharoen, N.; Li, R.; Prevelige, P. E.; Wang, Q. Polymer–virus core–shell structures prepared via co–assembly and template synthesis methods. *Sci. China Ser. B* **2010**, *53*, 71–77.

[31] Flynn, C. E.; Lee, S. W.; Peelle, B. R.; Belcher, A. M. Viruses as vehicles for growth, organization and assembly of materials. *Acta Mater.* **2003**, *51*, 5867–5880.

[32] Simons, G. F. M.; Konings, R. N. H.; Schoemakers, J. G. G. Genes-VI, genes-VII, and genes-IX of phage-M13 code for minor capsid proteins of the virion. *Proc. Nat. Acad. Sci. U. S. A.* **1981**, *78*, 4194–4198.

[33] Chiang, C. Y.; Mello, C. M.; Gu, J. J.; Silva, E.; Van Vliet, K. J.; Belcher, A. M. Weaving genetically engineered functionality into mechanically robust virus fibers. *Adv. Mater.* **2007**, *19*, 826–832.

[34] Nam, K. T.; Kim, D. W.; Yoo, P. J.; Chiang, C. Y.; Meethong, N.; Hammond, P. T.; Chiang, Y. M.; Belcher, A. M. Virus-enabled synthesis and assembly of nanowires for lithium ion battery electrodes. *Science* **2006**, *312*, 885–888.

[35] Niu, Z.; Bruckman, M. A.; Harp, B.; Mello, C. M.; Wang, Q. Bacteriophage M13 as a Scaffold for Preparing Conductive Polymeric Composite Fibers. *Nano Res.* **2008**, *1*, 235–241.

[36] Rong, J.; Lee, L. A.; Li, K.; Harp, B.; Mello, C. M.; Niu, Z.; Wang, Q. Oriented cell growth on self-assembled bacteriophage M13 thin films. *Chem. Commun.* **2008**, 5185–5187.

[37] Manchester, M.; Singh, P. Virus-based nanoparticles (VNPs): Platform technologies for diagnostic imaging. *Adv. Drug Deliv. Rev.* **2006**, *58*, 1505–1522.

[38] Yacoby, I.; Bar, H.; Benhar, I. Targeted drug-carrying bacteriophages as antibacterial nanomedicines. *Antimicrob. Agents Chemother.* **2007**, *51*, 2156–2163.

[39] Yacoby, I.; Shamis, M.; Bar, H.; Shabat, D.; Benhar, I. Targeting antibacterial agents by using drug-carrying filamentous bacteriophages. *Antimicrob. Agents Chemother.* **2006**, *50*, 2087–2097.

[40] Bar, H.; Yacoby, I.; Benhar, I. Killing cancer cells by targeted drug-carrying phage nanomedicines. *BMC Biotechnol.* **2008**, *8*, 37.

[41] Yacoby, I.; Benhar, I. Targeted filamentous bacteriophages as therapeutic agents. *Expert Opin. Drug Deliv.* **2008**, *5*,

321–329.
[42] Hilderbrand, S. A.; Kelly, K. A.; Weissleder, R.; Tung, C. H. Monofunctional near-infrared fluorochromes for imaging applications. *Bioconjugate Chem.* **2005**, *16*, 1275–1281.
[43] Hilderbrand, S. A.; Kelly, K. A.; Niedre, M.; Weissleder, R. Near infrared fluorescence-based bacteriophage particles for ratiometric pH imaging. *Bioconjugate Chem.* **2008**, *19*, 1635–1639.
[44] Li, K.; Chen, Y.; Li, S.; Nguyen, H. G.; Niu, Z.; You, S.; Mello, C. M.; Lu, X.; Wang, Q. Chemical modification of M13 bacteriophage and its application in cancer cell imaging. *Bioconjugate Chem.* **2010**, *21,* 1369–1377.
[45] Krag, D. N.; Shukla, G. S.; Shen, G. P.; Pero, S.; Ashikaga, T.; Fuller, S.; Weaver, D. L.; Burdette-Radoux, S.; Thomas, C. Selection of tumor-binding ligands in cancer patients with phage display libraries. *Cancer Res.* **2006**, *66*, 7724–7733.
[46] Yoo, H. S.; Park, T. G. Folate-receptor-targeted delivery of doxorubicin nano-aggregates stabilized by doxorubicin-PEG-folate conjugate. *J. Control. Release* **2004**, *100*, 247–256.
[47] Ganta, S.; Devalapally, H.; Shahiwala, A.; Amiji, M. A review of stimuli-responsive nanocarriers for drug and gene delivery. *J. Control. Release* **2008**, *126*, 187–204.
[48] Mammen, M.; Chio, S. K.; Whitesides, G. M. Polyvalent interactions in biological systems: Implications for design and use of multivalent ligands and inhibitors. *Angew. Chem. Int. Ed.* **1998**, *37*, 2755–2794.
[49] Miller, A. C.; Bershteyn, A.; Tan, W.; Hammond, P. T.; Cohen, R. E.; Irvine, D. J. Block copolymer micelles as nanocontainers for controlled release of proteins from biocompatible oil phases. *Biomacromolecules* **2009**, *10*, 732–741.
[50] Van Butsele, K.; Sibret, P.; Fustin, C. A.; Gohy, J. F.; Passirani, C.; Benoit, J. P.; Jérôme, R.; Jérôme, C. Synthesis and pH-dependent micellization of diblock copolymer mixtures. *J. Colloid Interf. Sci.* **2009**, *329*, 235–243.
[51] Saul, J. M.; Annapragada, A.; Natarajan, J. V.; Bellamkonda, R. V. Controlled targeting of liposomal doxorubicin via the folate receptor *in vitro*. *J. Control. Release* **2003**, *92*, 49–67.
[52] Ren, Y.; Wong, S. M.; Lim, L. Y. Folic acid-conjugated protein cages of a plant virus: A novel delivery platform for doxorubicin. *Bioconjugate Chem.* **2007**, *18*, 836–843.
[53] Francis, G. E.; Delgado, C. *Drug Targeting: Strategies, Principles, and Applications*; Humana Press/Totowa, New Jersey, 2000.
[54] Bala, I.; Bhardwaj, V.; Hariharan, S.; Sitterberg, J.; Bakowsky, U.; Kumar, M. Design of biodegradable nanoparticles: A novel approach to encapsulating poorly soluble phytochemical ellagic acid. *Nanotechnology* **2005**, *16*, 2819–2822.
[55] White, B.; Banerjee, S.; O'Brien, S.; Turro, N. J.; Herman, I. P. Zeta-potential measurements of surfactant-wrapped individual single-walled carbon nanotubes. *J. Phys. Chem. C* **2007**, *111*, 13684–13690.
[56] Lee, H. K.; Lee, H. Y.; Jeon, J. M. Codeposition of micro- and nano-sized SiC particles in the nickel matrix composite coatings obtained by electroplating. *Surf. Coat. Tech.* **2007**, *201*, 4711–4717.
[57] Butsele, K. V.; Fustin, C. A.; Gohy, J. F.; Jérôme, R.; Jérôme, C. Self-assembly and pH-responsiveness of ABC miktoarm star terpolymers. *Langmuir* **2008**, *25*, 107–111.
[58] Borchert, U.; Lipprandt, U.; Bilang, M.; Kimpfler, A.; Rank, A.; Peschka-Sass, R.; Schubert, R.; Lindner, P.; Farster, S. pH-induced release from P2VP–PEO block copolymer vesicles. *Langmuir* **2006**, *22*, 5843–5847.
[59] Gao, Y.; Chen, L.; Gu, W.; Xi, Y.; Lin, L.; Li, Y. Targeted nanoassembly loaded with docetaxel improves intracellular drug delivery and efficacy in murine breast cancer model. *Mol. Pharmaceut.s* **2008**, *5*, 1044–1054.
[60] Reddy, J. A.; Clapp, D. W.; Low, P. S. Retargeting of viral vectors to the folate receptor endocytic pathway. *J. Control. Release* **2001**, *74*, 77–82.
[61] Dube, D.; Francis, M.; Leroux, J. C.; Winnik, F. M. Preparation and tumor cell uptake of poly(*N*-isopropylacrylamide) folate conjugates. *Bioconjugate Chem.* **2002**, *13*, 685–692.
[62] Tian, Z.; Wang, M.; Zhang, A. Y.; Feng, Z. G. Preparation and evaluation of novel amphiphilic glycopeptide block copolymers as carriers for controlled drug release. *Polymer* **2008**, *49*, 446–454.